Conformational Difference between PDE4 Apoenzyme and Holoenzyme

France Laliberté, Yongxing Han, Arvind Govindarajan, André Giroux, Susana Liu, Brian Bobechko, Paula Lario, Adrienne Bartlett, Elise Gorseth, Michael Gresser, and Zheng Huang*

Department of Biochemistry and Molecular Biology, Merck Frosst Centre for Therapeutic Research, P.O. Box 1005, Pointe Claire-Dorval, Quebec, H9R 4P8, Canada

Received October 20, 1999; Revised Manuscript Received February 14, 2000

ABSTRACT: The type 4 cAMP-specific phosphodiesterases (PDE4s) are Mg^{2+}-dependent hydrolases that catalyze the hydrolysis of 3′,5′-cAMP to AMP. Previous studies indicate that PDE4 exists in two conformations that bind the inhibitor rolipram with affinities differing by more than 100-fold. Here we report that these two conformations are the consequence of PDE4 binding to its metal cofactor such as Mg^{2+}. Using a *f*luorescence *r*esonance *e*nergy *t*ransfer (FRET)-based equilibrium binding assay, we identified that L-791,760, a fluorescent inhibitor, binds to the apoenzyme (free enzyme) and the holoenzyme (enzyme bound to Mg^{2+}) with comparable affinities ($K_d \sim 30$ nM). By measuring the displacement of the bound L-791,760, we have also identified that other inhibitors bind differentially with the apoenzyme and the holoenzyme depending upon their structure. CDP-840, SB-207499, and RP-73401 bind preferentially to the holoenzyme. The conformational-sensitive inhibitor (*R*)-rolipram binds to the holoenzyme and apoenzyme with affinities (K_d) of 5 and 300 nM, respectively. In contrast to its high affinity ($K_d \sim 2$ μM) and active holoenzyme complex, cAMP binds to the apoenzyme nonproductively with a reduced affinity ($K_d \sim 170$ μM). These results demonstrate that cofactor binding to PDE4 is responsible for eliciting its high-affinity interaction with cAMP and the activation of catalysis.

3′,5′-Cyclic nucleotide phosphodiesterases (PDEs)[1] are families of divalent cation dependent hydrolases that catalyze the hydrolysis of cAMP and cGMP, and thereby terminate their roles as second messengers in mediating cellular responses to various hormones and neurotransmitters. Ten families of PDE enzymes, sharing a conserved catalytic domain (∼270 amino acids) and exhibiting distinct substrate specificity and regulatory properties, have been identified (*1, 2*). Most PDEs are encoded by multiple genes to produce isoenzymes within each family with distinct regulatory properties and intracellular localization. It has been proposed that this diversity, together with multiple adenylate cyclases (AC) coupled with the different families of protein kinase A and G anchoring proteins, provides the complex network and specificity required for transducing the cAMP- and cGMP-mediated signals (*3*−*5*).

The cAMP-specific type 4 phosphodiesterases (PDE4s) have been the focus of considerable attention following the recognition that they are the primary enzymes responsible for the metabolism of cAMP in inflammatory and immune cells (*6*). In humans, they are encoded by four genes (4A, 4B, 4C, and 4D) with each producing a series of isoenzymes through alternative mRNA splicing and differential promoter usage. A unique N-terminal region with a common C-terminal and catalytic domain distinguishes the variants within each isoform. The 'long' variants are characterized by the presence of two *u*pstream *c*onserved *r*egions, UCR1 and UCR2, that connect them to the common catalytic domain via two linker regions, LR1 (linking UCR1 to UCR2) and LR2 (linking UCR2 to the catalytic domain). The 'short' variants lack the UCR1 domain (*7*). In addition to their involvement in protein targeting and membrane anchoring (*7*−*10*), the UCR1 of PDE4D3 also provides the conserved Arg-Arg-Glu-Ser (RRES) motif for PKA-mediated serine phosphorylation and activation by an increased affinity for the cofactor Mg^{2+} (*11, 12*). Conversely, the Erk2-mediated serine phosphorylation at the conserved Ser-Pro-Ser (SPS) motif near the C-terminal region of the catalytic domain of PDE4D3 inhibits its catalytic activity (*13*). Despite the increased understanding of the tissue-specific expression of different PDE4 isoforms, their biological functions remain elusive (*10, 14, 15*).

The complexity of PDE4 gene products may provide an explanation for the wide variety of physiological consequences of their inhibition. Over the years, several PDE4 inhibitors have been shown to be antiinflammatory in vivo. Therefore, they represent a promising new class of agents for the treatment of various inflammatory diseases such as asthma (*6*). However, early clinical trials with inhibitors, such as rolipram, proved inconclusive due to dose-limiting side

* To whom correspondence should be addressed at the Department of Biochemistry and Molecular Biology, Merck Frosst Centre for Therapeutic Research, P.O. Box 1005, Pointe Claire-Dorval, Quebec, H9R 4P8, Canada. Fax: (514) 695-0693; Tel: (514) 428-3143; E-mail: zheng_huang@merck.com.

[1] Abbreviations: cAMP, 3′,5′-cyclic adenosine monophosphate; CDP-840, (*R*)-(+)-4-[2-(3-cyclopentyloxy-4-methoxyphenyl)-2-phenylethyl]pyridine; FRET, fluorescence resonance energy transfer; GST, glutathione-*S*-transferase; L-791,760, 4-[5-(3,4-dimethoxyphenyl)-3-{[(4,6-dimethyl-2-pyrimidinyl)sulfanyl] methyl}-2-thienyl]benzenesulfonamide; PDE, 3′,5′-cyclic nucleotide phosphodiesterase; PDE4, type 4 phosphodiesterase; rolipram, 4-[3-(cyclopentoxyl)-4-methoxyphenyl]-2-pyrrolidone; RP-73401, 3-cyclopentyloxy-*N*-(3,5-dichloro-4-pyridil)-4-methoxybenzamide; RS-14203, 6-(4-pyridylmethyl)-8-(3-nitrophenyl)guinoline; SB-207499 (Ariflo), *cis*-4-[cyano-4-(3-cyclopentyloxy-4-methoxyphenyl-(*R*)-1-cyclohexane]carboxylic acid; UCR, upstream conserved region.

10.1021/bi992432w CCC: $19.00 © 2000 American Chemical Society
Published on Web 05/04/2000

effects such as nausea and emesis (*16, 17*). Recently, clinical efficacy was reported for SB-207499 (Ariflo, SmithKline Beecham) in asthmatics and patients with COPD (chronic obstructive pulmonary disease) at doses below the occurrence of significant side effects, indicating that an increased therapeutic window can be achieved for PDE4 inhibitor (*18*).

Despite significant advances in developing potent and selective PDE4 inhibitors, an important issue remains to be clarified regarding their multiphasic interaction with PDE4. Along with inhibiting PDE4-mediated cAMP hydrolysis, some PDE4 inhibitors have been found to interact with the same enzyme with different affinities as typified by (*R*)-rolipram. Under similar conditions, (*R*)-rolipram has been reported to bind to PDE4 with a high affinity (1 to 5 nM K_d) and a low stoichiometry, while its potency on inhibiting catalysis with the same enzyme varied with enzyme source and sample batch from 5 to 1000 nM (*19*−*23*). Results from mutational studies, especially the mapping of rolipram-sensitive mutations within a region of ∼70 residues in the C-terminal end of the catalytic domain (*20, 21, 24*−*26*), and the simultaneous detection of 1 and 500 nM (*R*)-rolipram binding within the PDE4B catalytic domain support the hypothesis that the high-affinity rolipram binding site represents one of two coexisting conformations of the PDE4 active site (*27, 28*).

To better understand PDE4 catalysis and its inhibition, we designed L-791,760, a highly fluorescent and active-site-directed PDE4 inhibitor (*29*). Utilizing its optimized fluorescence property, a fluorescence resonance energy transfer (FRET)-based equilibrium PDE4 binding assay was developed to monitor cAMP and inhibitor binding to both the PDE4 apoenzyme (free enzyme) and the PDE4 holoenzyme (enzyme bound to Mg^{2+}) independent of catalysis. Here we report the characterization of this novel assay and the observation that the transition of PDE4 from its apoenzyme to the holoenzyme is responsible for the high-affinity binding of cAMP and the differential binding of some PDE4 inhibitors.

MATERIALS AND METHODS

Chemicals. Analytical grade HEPES, EDTA, and cAMP and ultra grade $MgCl_2$ and KCl were from Sigma/Aldrich. [^{3}H]-cAMP, [2,8-^{3}H]-cyclic adenosine 3′,5′-monophosphate, was from Amersham International Inc. PDE4 inhibitors [SB-207499, RP-73401, (*R*)-rolipram, and RS-14203] were prepared at Merck Frosst. CDP-840 was from Celltech. L-791,760 was prepared according to the procedure described (*29*). Its spectral properties are as follows: ^{1}H NMR (acetone-d_6), 8.00 (d, 2H), 7.80 (d, 2H), 7.53 (s, 1H), 7.25 (d, 1H), 7.21 (dd, 1H), 7.00 (d, 1H), 6.90 (s, 1H), 6.64(bs, 2H, NH_2), 4.5 (s, 2H), 3.89 (s, 3H), 3.84 (s, 3H), 2.33 (s, 6H); mass spectrum 528.4 $(M+1)^+$ (APCI).

Absorbance and Fluorescence Spectra. The fluorescence spectrum and the 90° light scattering were measured on an LS-50B spectrophotometer (Perkin-Elmer) equipped with four stirred quartz cuvettes. The absorbance spectrum was recorded on a Cary UV-spectrometer (Varian). All experiments were conducted at room temperature (∼23 °C).

PDE4 Enzyme. Recombinant human PDE4A$^{248-886}$ was expressed as a GST fusion protein in a baculovirus/SF9 cell expression system and purified to homogeneity as previously described (*21, 22*). After elution with 5 mM glutathione from the glutathione−Sepharose beads, the fusion protein was concentrated and further purified on a Mono-Q column using a 0−1 M KCl linear gradient in a buffer containing 20 mM HEPES (pH 7.2), 1 mM EDTA, 1 mM DTT, and 10% (v/v) glycerol. The resulting GST-PDE4A^{248}, homogeneous on SDS−PAGE, had a specific activity (V_{max}) for cAMP hydrolysis at 5−10 μmol mg^{-1} min^{-1} in the presence of 10 mM Mg^{2+}, a K_m of 2 μM, and an EC_{50} of 100 μM for Mg^{2+} at 0.1 μM cAMP. The same K_m and V_{max} for cAMP hydrolysis and similar catalytic potency for inhibitors listed were observed between the fusion protein and its PDE4A^{248} fragment, which was obtained by cleaving the fusion protein with a catalytic amount of thrombin. The fusion protein was stored at −80 °C in a buffer containing 20% (v/v) glycerol, 1 mM EDTA, 1 mM DTT, 20 mM HEPES (pH 7.5), and 200 mM KCl. Protein concentration was determined by its A_{280} reading using an extinction coefficient of 1.0 mg^{-1} mL^{-1} cm^{-1} calculated according to the method of Perkins (*30*). PDE4A$^{1-886}$ from SF9 cells, purified using the same EDTA-containing HPLC elution buffer at its last purification step, had insignificant amounts (<0.1 mol fraction) of divalent cations from direct metal ion analysis (*31*).

PDE Activity Assay. PDE4 catalytic activity in the presence of Mg^{2+} was monitored by measuring the hydrolysis of [^{3}H]-cAMP to [^{3}H]-AMP as previously described using a PDE-SPA kit from Amersham International (*31*). The typical assay mixture (190 μL) contains 105 nM [^{3}H]-cAMP (1 μCi/mL) in the assay buffer (20 mM HEPES, 10 mM $MgCl_2$, 1 mM EDTA, 100 mM KCl, pH 7.5) and 2 μL of test compound in DMSO [the final DMSO concentration, 1% (v/v), was below its inhibitory concentration of ≥4%]. Hydrolysis of [^{3}H]-cAMP was initiated by the addition of 10 μL of GST-PDE4A^{248} (∼50 pM final concentration) at 30 °C. The reaction was terminated after 10 min (with ∼10% substrate conversion) by the addition of 50 μL of PDE-SPA beads. [^{3}H]-AMP, captured by the SPA beads, was quantified on a Wallac-Microbeta scintillation counter. A linear reaction progress curve (up to 30 min) and a linear enzyme concentration response (from 0 to 500 pM) were observed with respect to product generation under these conditions. The IC_{50} value of an inhibitor was calculated from a 11-point dose−response curve performed in duplicate using a 4-parameter least-squares nonlinear regression fit. The IC_{50} values were the average of ≥3 experiments unless otherwise stated. The relationship between the binding affinities of inhibitors to PDE4 apoenzyme and holoenzyme and their IC_{50} values in catalysis inhibition will be presented and discussed in a separate report.

L-791,760 Aqueous Solubility. L-791,760, soluble in organic solvents such as methanol or DMSO, has an absorption λ_{max} at 340 nm and an extinction coefficient of 20 000 AU·cm^{-1}·M^{-1} in methanol. Its solubility is limited in aqueous solution due to hydrophobicity. The presence of L-791,760 aggregates was detectable in the assay buffer when its total concentration exceeded ∼200 nM, leading to an increased 90° light scattering at 400 nm. These aggregates became visible when its total concentration exceeded ∼2 μM. The presence of aggregates below 200 nM, less sensitive toward the 400 nm light, was inferred from an increased and scattered nonspecific FRET signal when its concentration exceeded ∼80 nM. A stable L-791,760 solution (∼60 nM)

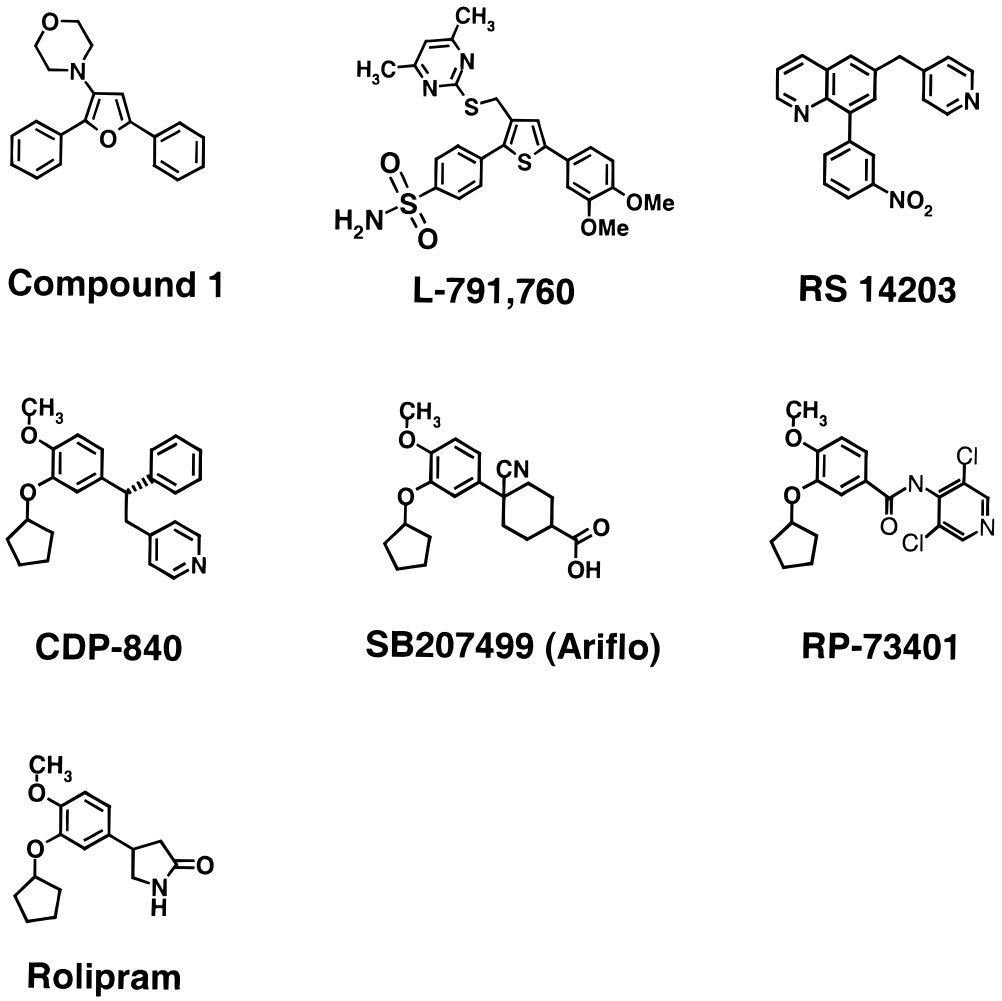

FIGURE 1: Inhibitor structures.

was obtained by dissolving 100 nM L-791,760 in the assay buffer and equilibrated for 18 h at room temperature. Its concentration was determined by measuring the fluorescence intensity of 100 μL of the sample in 900 μL of 80% (v/v) methanol/buffer against a standard curve (excitation, 340 nm; emission, 465 nm). Samples with different amounts of L-791,760 were prepared from this stock solution with each concentration verified using the standard curve.

FRET-Based PDE4 Equilibrium Binding Assay. The typical assay solution (1 mL) contained 5−10 nM GST-PDE4A^{248}, 30 nM L-791,760, 10 mM EDTA (for apoenzyme) or 5 mM $MgCl_2$ (for holoenzyme), 130 mM KCl, and 20 mM HEPES (pH 7.5). FRET intensity was recorded by monitoring the emission at 465 nm (slit width 10 nm) with the selective excitation of PDE4 at 285 nm (slit width 5 nm). Inhibitor was added via 5 μL of DMSO. The presence of 0.5% (v/v, final) DMSO had a minimal effect on the FRET intensity and the catalytic activity of PDE4. The FRET intensity derived from the L-791,760/PDE4 binding was obtained by subtracting the total fluorescence at 465 nm from the residual emission of L-791,760 due to its direct excitation at 285 nm. Specific FRET intensity, resulting from L-791,760 binding to the PDE4 active site, was defined as the portion of the FRET intensity (~90%) which was eliminated in the presence of saturating concentration of RS-14203 (70 nM). IC_{50} values of PDE4 inhibitors were determined using a 4-parameter least-squares nonlinear regression fit of inhibitor concentration vs percent specific FRET intensity. The limited solubility of L-791,760 in buffer prevented the direct measurement of the K_d value of a competing ligand by varying its concentration. The K_d value of a competing ligand was estimated from the formula: $K_d = IC_{50}/(1 + [\text{L-791,760}]/K_d^{\text{L-791,760}})$ assuming a competitive binding with L-791,760.

cAMP Binding to PDE4 Apoenzyme and Holoenzyme. For cAMP binding to PDE4 apoenzyme, 1.5 μg of GST-PDE4A^{248} (in a 15 μL buffer solution containing 10 mM EDTA) was added to a 1 mL stirred solution containing 10 mM EDTA, cAMP (from 0 to 1.6 mM), 30 nM L-791,760, 130 mM KCl, and 20 mM HEPES (pH 7.2). High cAMP concentrations (>100 μM) reduced the intrinsic fluorescence of L-791,760 (4% reduction at 100 μM and 40% reduction at 1.6 mM cAMP) due to its absorbance of the excitation light. The specific FRET intensities displaced by cAMP were corrected for the quenching effect when cAMP concentrations exceeded 100 μM, assuming an identical quenching efficiency. For cAMP binding to PDE4 holoenzyme, GST-PDE4A^{248} holoenzyme (1.5 μg in a 15 μL buffer containing 10 mM Mg^{2+}) was added to a 1 mL solution containing 5 mM $MgCl_2$, cAMP (up to 100 μM), 30 nM L-791,760, 50 μM EDTA, 130 mM KCl, and 20 mM HEPES at pH 7.5. ΔFRET intensity was determined by subtracting the final FRET intensity from the initial intensity. The delay time was the duration to recover 50% of the ΔFRET intensity. No quenching correction below 100 μM cAMP was made to

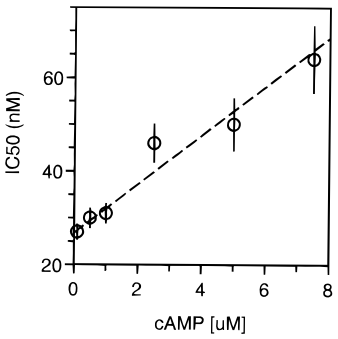

FIGURE 2: Inhibition of PDE4 catalysis by L-791,760 with respect to increased cAMP concentration. The IC_{50} values (average of 3 experiments) were determined in the presence of 0.05 nM GST-PDE4A^{248} and 10 mM Mg^{2+}. Linear regression analysis gave an intercept of 27 (±3) nM and a slope of 5 (±1) nM L-791,760/μM cAMP.

the ΔFRET intensities due to its insignificance (≤4% reduction). To minimize estimation error, the delay time at 100 μM cAMP was used to calculate the turnover number of cAMP.

RESULTS

L-791,760 Is a Highly Fluorescent and Competitive PDE4 Inhibitor. To gain a better understanding of PDE4 catalysis and its inhibition, we recently prepared L-791,760, a highly fluorescent and potent PDE4 inhibitor. L-791,760 was derived from an initial screening lead, compound **1** (Figure 1), a furan derivative, which inhibits cAMP hydrolysis with an IC_{50} of 2.5 μM at 0.1 μM cAMP (*32*). Modifications using a novel three-dimensional combinatorial chemistry approach around compound **1** led to the identification of a class of substituted thiophene derivatives with significantly improved potencies, many of which were highly fluorescent (*29*). This led to the discovery of L-791,760. Shown in Figure 2 is the effect of the cAMP concentration on its IC_{50} values for the inhibition of the PDE activity of GST-PDE4A^{248}. A linear relationship was observed with a slope of 5 nM L-791,760/μM cAMP and an intercept at 27 nM. The result supports that L-791,760 is a competitive PDE4 inhibitor.

The delocalized structure of L-791,760 resulted in its strong absorbance near 340 nm [extinction coefficient (ϵ) of 20 000 $cm^{-1}\cdot M^{-1}$ in methanol], which overlapped well with the PDE4 intrinsic fluorescence [Figure 3: emission spectra of GST-PDE4A^{248} (B) compared with the excitation spectra of L-791,760 (C)]. The excited state of L-791,760 decayed exclusively via fluorescence in high quantum yield with an emission $\lambda_{max} \sim 475$ nm in aqueous buffer (E in Figure 3). The combination of its high absorbance and a near-quantitative fluorescence quantum yield permitted the detection of as low as 1 nM L-791,760. In addition, no significant photobleaching was detected after 12 h of continuous excitation, indicating that L-791,760 was stable photochemically.

L-791,760 Binds Specifically to PDE4 Apoenzyme and Holoenzyme. The maximal spectral overlap between the PDE4 intrinsic fluorescence and the absorbance spectrum of L-791,760 permitted the development of a sensitive FRET-based equilibrium PDE4 binding assay. The assay utilizes the fact that fluorescence resonance energy transfer decays rapidly with increased distance between the donor and

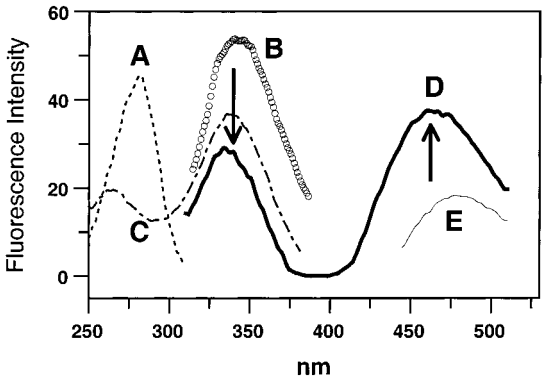

FIGURE 3: Fluorescence spectra of L-791,760, GST-PDE4A^{248}, and their mixture. (A) Excitation spectrum of GST-PDE4A^{248} (~25 nM) with emission at 340 nm (dashed line); (B) emission spectrum of GST-PDE4A^{248} with excitation at 285 nm (○); (C) excitation spectrum of L-791,760 (30 nM) with emission at 475 nm (dashed line); (D) emission spectrum of the solution containing L-791,760 and GST-PDE4A^{248} with excitation at 285 nm (solid line, complex is the major species here); (E) emission spectra of L-791,760 with excitation at 285 nm (thin solid line). A blue-shift from a λ_{max} of 475 nm (in E) to a λ_{max} of 465 nm (in D) accompanied the binding of L-791,760 to PDE4. The fluorescence resonance energy transfer between L-791,760 and PDE4 led to an increased emission at 465 nm (difference between D and E near 465 nm) and a decreased emission of PDE4 near 340 nm (the difference between B and D at 340 nm) as marked by the arrows. The background spectrum from the buffer alone has been subtracted from each trace.

acceptor (the transfer efficiency is proportional to $1/r^6$) and thus only occurs efficiently between the excited state of PDE4 and its bound ligand (*33*). When PDE4 was selectively excited at 285 nm, a fluorescence resonance energy transfer occurred from the excited state of PDE4 to the bound L-791,760, leading to an increased emission centered at 465 nm from the bound L-791,760 and a decreased emission near 340 nm from the bound PDE4 as marked by the arrows in Figure 3 [comparing the emission spectra of GST-PDE4A^{248} (B), of L-791,760 (E), of the solution containing the complex (D), all with excitation at 285 nm]. Therefore, the fluorescence at 465 nm with excitation at 285 nm (D in Figure 3) was composed of (a) the FRET intensity due to the energy transfer from the excited PDE4 to its bound L-791,760, and (b) the intrinsic fluorescence of L-791,760 from excitation at 285 nm (E in Figure 3). The PDE4-induced FRET intensity was dose-dependently reduced by the presence of RS-14203, a competitive PDE4 inhibitor (*34*) with an IC_{50} value of 0.07 nM in inhibiting the catalytic activity of GST-PDE4A^{248} at 0.1 μM cAMP (Table 1). The addition of GST-PDE4A^{248} (5 nM) to a solution (1 mL) containing 30 nM L-791,760 and 10 mM EDTA resulted in an instantaneous increase in fluorescence at 465 nm due to the rapid formation of a L-791,760/PDE4 apoenzyme complex (Figure 4). The addition of RS-14203 at point B (via 5 μL of DMSO) rapidly decreased the PDE4-induced FRET intensity in a dose-dependent manner (RS-14203 binding to PDE4 had no effect on the PDE4 intrinsic fluorescence in the absence of L-791,760; the fluorescence of L-791,760 was not affected by RS-14203; and DMSO introduced a negligible perturbation of the fluorescence intensity). Over 90% of the FRET intensity was eliminated in the presence of a saturating concentration of RS-14203 (70 nM), with the remaining portion insensitive toward any inhibitor tested in the presence or absence of Mg^{2+} as marked in Figure 4. The inhibitor-insensitive

Table 1: Potency of Inhibitors on Catalysis and Their Apoenzyme and Holoenzyme Affinities[a]

inhibitors	apoenzyme affinity (IC_{50}, nM)	holoenzyme affinity (IC_{50}, nM)	catalytic potency (IC_{50}, nM)
compound **1**	ND	ND	2500
L-791,760	$K_d = 27$ (±5)	$K_d = 30$ (±5)	30 (±15)
CDP-840	>5000	10 (±5)	4 (±2)
SB-207499	>5000	100 (±30)	45 (±15)
RP-73401	>5000	≤5 (assay limit)	0.3 (±0.2)
(*R*)-rolipram	600 (±200)	10 (±5)	5 (±3)
RS-14203	≤5 (assay limit)	≤5 (assay limit)	0.07 (±0.05)

[a] Apoenzyme and holoenzyme affinities (IC_{50} ± SEM) were the average of 3 experiments using 5 nM GST-PDE4A^{248}, 30 nM L-791,760, 10 mM EDTA (apoenzyme), or 5 mM Mg^{2+}(holoenzyme). The corresponding K_d values were estimated at 50% of the IC_{50} values since the concentration of L-791,760 was close to its estimated K_d. Both apparent IC_{50} values for RS-14203 were at the detection limit of the FRET assay. The K_d values of L-791,760 were estimated from its binding curves in Figure 5. Catalytic potencies (IC_{50} ± SEM) were the average of ≥4 experiments using 0.05 nM GST-PDE4A^{248}, 0.1 μM cAMP, and 10 mM Mg^{2+}.

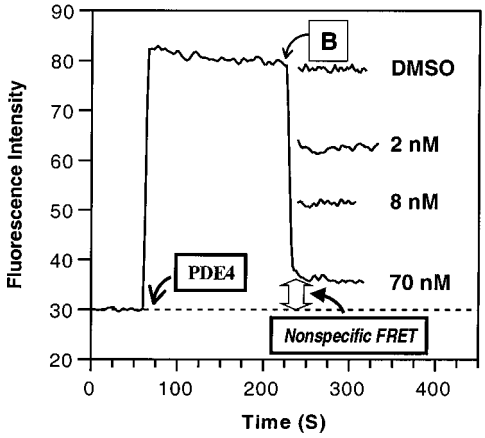

FIGURE 4: Formation of a PDE4 apoenzyme/L-791,760 complex monitored by the FRET assay. Total fluorescence intensity is displayed. Addition of GST-PDE4A^{248} apoenzyme (~5 nM) to a solution containing 30 nM L-791,760 and 10 mM EDTA at ~70 s resulted in a rapidly increased emission at 465 nm from 30 to ~84 intensity units (excitation at 285 nm). RS-14203 (introduced at point B) dose-dependently and rapidly reduced the specific FRET intensity. 0.5% (v/v) DMSO had a minimal effect. The nonspecific portion of the FRET intensity (~5 units) was insensitive toward further increases in RS-14203 concentration or the presence of other inhibitors.

(nonspecific) FRET signal could be derived from the binding of L-791,760 to either the GST domain or the PDE4 domain outside its active site (nonspecific FRET signals were observed between L-791,760 and GST or BSA). In addition to the efficient fluorescence resonance energy transfer, the binding of L-791,760 to PDE4 also induced a detectable blue-shift in its emission spectrum from a λ_{max} ~475 nm to ~465 nm, consistent with the change of its surrounding environment from a polar aqueous buffer to a more hydrophobic protein binding pocket (*33*).

Shown in Figure 5 are the dose−response curves of the specific (● with Mg^{2+} and ○ with EDTA) and the nonspecific (▲ with Mg^{2+} and △ with EDTA) FRET intensities with respect to increased L-791,760 concentration in the presence or absence of 5 mM Mg^{2+}. Below 45 nM L-791,-760, the FRET intensities were almost exclusively (>90%) derived from its specific binding to PDE4 apoenzyme or

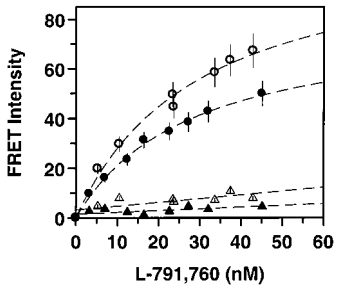

FIGURE 5: L-791,760 binding to PDE4 apoenzyme and holoenzyme. Apoenzyme (5 nM GST-PDE4A^{248} in 10 mM EDTA) and holoenzyme (in 5 mM Mg^{2+}) were mixed with increasing concentrations of L-791,760. The nonspecific FRET intensities (△, EDTA; ▲, Mg^{2+}, insensitive to the presence of 70 nM RS-14203) were linear with respect to increasing L-791,760 concentration up to 45 nM. The specific FRET intensities, ○ (EDTA) and ● (Mg^{2+}), became less reproducible above 60 nM L-791,760. Nonlinear regression analysis of the specific FRET intensities gave a K_d of 27 (±5) nM and a ΔF_{max} of 110 (±10) units for its apoenzyme binding and a K_d of 30 (±5) nM and a ΔF_{max} of 80 (±10) units for its holoenzyme binding.

holoenzyme, and both were nearly eliminated by the presence of a saturating concentration of RS-14203 (70 nM). The nonspecific FRET intensities increased linearly and accounted for less than 10% of the total FRET intensity. Saturation binding analysis of the specific FRET intensity, which increased monophasically with increased concentrations of L-791,760, gave estimated K_d values of 27 and 30 nM with a Hill coefficient close to 1 for both its apoenzyme and its holoenzyme binding. Above 60 nM L-791,760, the FRET intensities became less reproducible and were associated with increased and scattered nonspecific FRET intensities. This was likely due to the contribution from the nonspecific binding of the fusion protein with L-791,760 aggregates. Their presence was detectable by an increased 90° light scattering at 400 nm when the total L-791,760 concentration exceeded 200 nM (the particles became visible above ~2 μM). Thus, concentrations of L-791,760 from 20 to 40 nM and GST-PDE4A^{248} (≥5 nM) were typically used to evaluate the competing binding of other inhibitors to ensure a robust dynamic range with a good detection limit. Under these conditions, a signal-to-noise ratio of >5:1 was typically achieved.

Differential Binding of Inhibitors with PDE4 Apoenzyme and Holoenzyme. By monitoring the displacement of the bound L-791,760 from its apoenzyme or holoenzyme complex, we identified that other PDE4 inhibitors interact differentially with the apoenzyme and holoenzyme depending upon their structures (see Table 1). CDP-840 (Figure 6A), SB-207499, and RP-73401, competitive inhibitors with respect to cAMP (*19*, *22*, *23*), competed with the holoenzyme binding of L-791,760, yielding IC_{50} values at 10, 100, and ≤5 nM, respectively. These IC_{50} values corresponded to K_d ~ 5 nM for CDP-840, K_d ~ 50 nM for SB-207499, and K_d ≤ 5 nM for RP-73401 for their holoenzyme interactions after taking into account (a) the L-791,760 concentration used was near its K_d and (b) the 5 nM detection limit of the assay due to the presence of ~5 nM PDE4. In the presence of 10 mM EDTA, less than 30% of the specific FRET intensity from the apoenzyme binding of L-791,760 was displaced by either 10 μM SB-207499, 10 μM CDP-840, or 10 μM RP-73401, demonstrating that they bind preferentially to the holoenzyme.

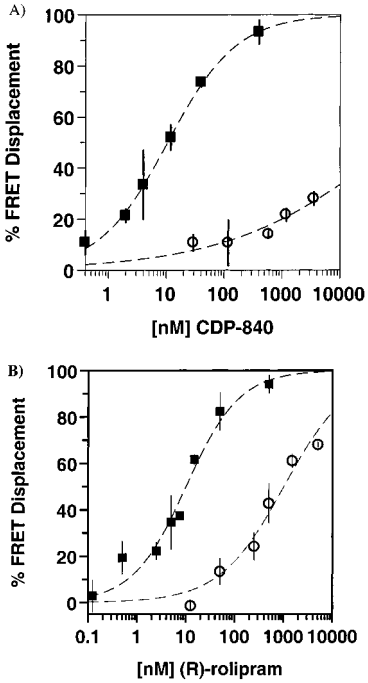

FIGURE 6: Displacement of the bound L-791,760 from the apoenzyme (○) and the holoenzyme (■) by CDP-840 (A) and (*R*)-rolipram (B). The data were the average of 3 experiments. The IC_{50} values were as follows: CDP-840, 10 (±5) nM for holoenzyme and >5000 nM for apoenzyme; (*R*)-rolipram, 10 (±5) nM for holoenzyme and 600 (±200) nM for apoenzyme.

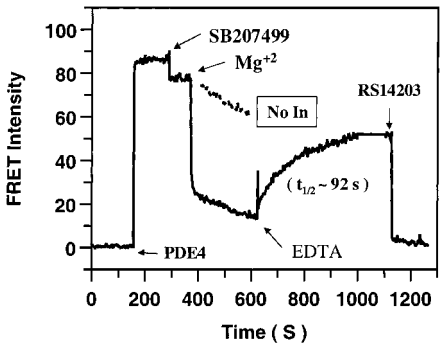

FIGURE 7: Time course of Mg^{2+}-induced association of SB-207499 with the holoenzyme and its dissociation triggered by EDTA. GST-PDE4A^{248} apoenzyme (~15 nM) was added to a 1 mL buffer solution containing 30 nM L-791,760 and 1 mM EDTA at ~170 s. SB-207499 (200 nM) was added at ~300 s. Mg^{2+} (2 mM final, net [Mg^{2+}] ~1 mM) was added at ~380 s. 10 mM EDTA (final concentration) was added at ~630 s. The FRET recovery followed a first-order process with a $t_{1/2}$ of 92 s. RS-14203 (200 nM) was added at ~1150 s. The dashed line marked "No In" was the fluorescence decay time course in the absence of SB-207499 after the addition of Mg^{2+}. It was caused by an irreversible loss of PDE4 to the cuvette surface.

The near-exclusive binding of SB-207499 to PDE4 holoenzyme provided the opportunity to monitor its dissociation triggered by the removal of Mg^{2+} as illustrated in Figure 7. A L-791,760/apoenzyme complex was formed instantaneously after the addition of GST-PDE4A^{248} (at ~170 s) to a buffer solution containing 30 nM L-791,760 and 1 mM EDTA. The addition of SB-207499 (200 nM at ~300 s) resulted in a small decrease of the FRET intensity due to its weak affinity with the apoenzyme. The addition of Mg^{2+} (2 mM at ~ 380 s) triggered a rapid decrease in the FRET intensity due to the competing formation of the high-affinity SB-207499/holoenzyme complex. Mg^{2+} alone, in the absence of SB-207499, induced a slow decay of the FRET intensity as illustrated by the dashed line marked "No In". This was traced to a gradual and irreversible loss of PDE4 to the surface of the quartz cuvette, which was confirmed by a parallel loss of PDE activity and PDE4 in the solution by Western analysis (the loss of PDE4 to the cuvette surface could be reduced with the use of an increased amount of PDE4). The addition of excess EDTA (10 mM at ~630 s) resulted in a first-order recovery of the FRET intensity with a half-life of ~92 s. After taking into account the reduced window from the loss of protein, the FRET signal displaced by SB-207499 in the presence of Mg^{2+} was quantitatively recovered. This was consistent with the disruption of the SB-207499/holoenzyme complex and the formation of a L-791,-760/apoenzyme complex due to the loss of Mg^{2+}. The relatively slow transition would suggest that the Mg^{2+} dissociation was rate-limiting. Saturating concentration of RS-14203 (200 nM) was added near the end of the time course to confirm the specificity of the FRET intensity.

In contrast to the near-exclusive holoenzyme binding of CDP-840, SB-207499, and RP-73401, (*R*)-rolipram competed with both the holoenzyme and the apoenzyme binding of L-791,760 with IC_{50} values of 10 and 600 nM, corresponding to K_d values of 5 and 300 nM, respectively (Figure 6B). RS-14203, its structure differing significantly from the others, had high affinities for both PDE4 apoenzyme and holoenzyme with the apparent IC_{50} values at the 5 nM assay detection limit. Thus, its holoenzyme and apoenzyme affinities could be below 5 nM.

Selective and Productive Binding of cAMP to PDE4 Holoenzyme. In addition to the structure-dependent differential binding of inhibitors, cAMP binds selectively to the PDE4 holoenzyme. In the absence of Mg^{2+}, the formation of a low-affinity cAMP/PDE4 apoenzyme complex was detected as illustrated by the dose-dependent displacement of the FRET intensity by cAMP (Figure 8A). The presence of high cAMP concentrations (>100 μM), in addition to its specific competition, also led to a reduced fluorescence due to the absorbance of the excitation light at 285 nm by cAMP. After correcting for the quenching effect, an IC_{50} value of 340 μM was detected for cAMP binding to the apoenzyme (Figure 8C, ○). This translated to a K_d ~ 170 μM for cAMP after taking into account the presence of 30 nM L-791,760. On the other hand, when PDE4 holoenzyme was added to solutions containing cAMP in the presence of Mg^{2+}, the FRET intensity of the holoenzyme/L-791,760 complex was potently displaced by cAMP initially (Figure 8B). However, the rapid depletion of cAMP, due to its hydrolysis to AMP, resulted in the recovery of the FRET intensity due to an increased formation of the holoenzyme/L-791,760 complex. Thus, the ΔFRET intensity reflected the occupancy of the PDE4 active site by cAMP with the recovery duration representing the time needed for the near-complete hydrolysis of cAMP. It took ~430 s to hydrolyze 1 mL of 100 μM cAMP (100 nmol) by 15 pmol of PDE4 holoenzyme, which translated to a turnover number of 15 s^{-1} for cAMP hydrolysis. From the ΔFRET intensity/cAMP response curve in Figure 8C (●), an IC_{50} value of 3.8 μM was obtained, translating to a K_s ~ 1.9 μM for cAMP binding to the PDE4 holoenzyme.

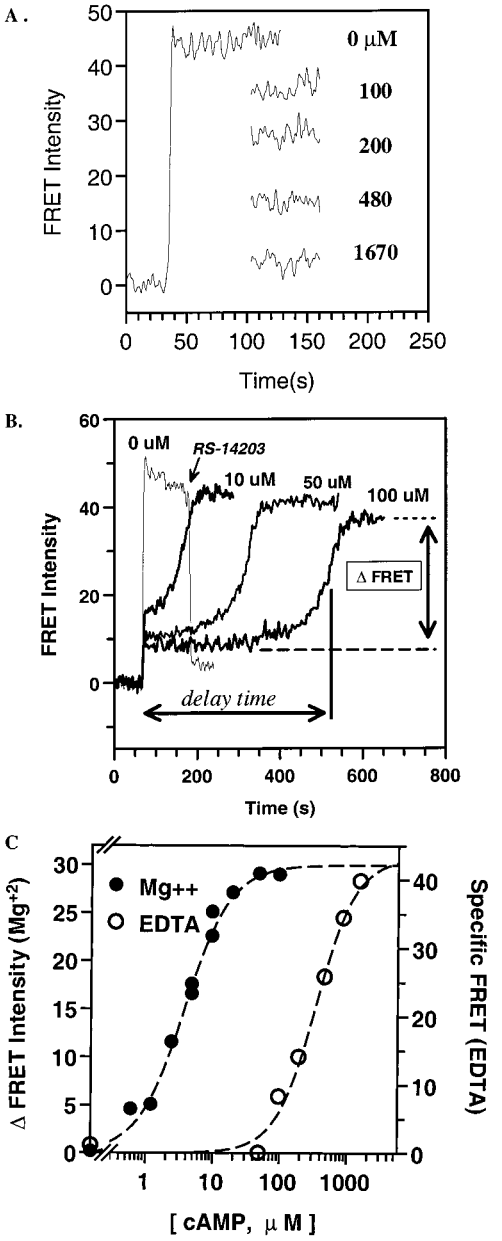

FIGURE 8: cAMP binding to PDE4 apoenzyme and holoenzyme and its hydrolysis monitored by the FRET binding assay. (A) Apoenzyme (1.5 μg of GST-PDE4A^{248} in 10 mM EDTA) was added to solutions containing 30 nM L-791,760, 10 mM EDTA, and increasing concentrations of cAMP. The specific FRET intensities displaced by cAMP, after correcting for its quenching effect above 100 μM (see Materials and Methods for detail), were used to estimate its IC_{50} in panel C. (B) Holoenzyme (1.5 μg of GST-PDE4A^{248} in 5 mM Mg^{2+}) was added to solutions containing 30 nM L-791,760, 5 mM Mg, and increasing concentrations of cAMP at ~70 s. Excess RS14203 (70 nM) was added to the solution containing 0 μM cAMP at ~190 s to define the specific FRET window. The time to recover 50% of the ΔFRET intensity was ~430 s at 100 μM cAMP, which corresponded to a turnover of 15 s^{-1} for cAMP hydrolysis. (C) Dose−response curves of the specific FRET intensities displaced by cAMP in the presence of 10 mM EDTA (○) and the ΔFRET intensities in the presence of 5 mM Mg^{2+} (●). The IC_{50} values of cAMP binding to GST-PDE4A^{248} were 3.8 (±0.4) μM in the presence of Mg^{2+} and 340 (±45) μM in the presence of EDTA with a near-unity Hill coefficient for both curves.

DISCUSSION

The results presented here demonstrate that the active site of PDE4 apoenzyme and holoenzyme exists in two different conformational states. Mg^{2+} binding to PDE4 is responsible for eliciting its high-affinity interaction with cAMP, the activation of catalysis, and the differential binding of inhibitor. CDP-840, SB-207499, and RP-73401 bind preferentially to the holoenzyme, whereas L-791,760, (*R*)-rolipram, and RS-14203 bind to both holoenzyme and apoenzyme as illustrated by the scheme in Figure 9. The affinities of the inhibitors for the apoenzyme and holoenzyme are summarized in Table 1 together with their potencies on the catalytic activity of GST-PDE4A^{248}. Their inhibitory potencies on catalysis at saturating Mg^{2+} concentration (10 mM Mg^{2+} compared with its EC_{50} of 0.1 mM) mirrored their holoenzyme affinities from the FRET assay except for RP-73401 and RS-14203, whose inhibitory potencies of 0.3 and 0.07 nM were below the detection limit of the FRET assay. The apoenzyme and holoenzyme affinities of cAMP and its catalytic turnover from the FRET assay are summarized in Table 2, together with its K_m and k_{cat} determined by measuring [^{3}H]-cAMP hydrolysis. Its binding affinity of 1.9 μM (K_s) with the holoenzyme was similar to its K_m of 2 μM from activity measurement. In addition, the turnover number for cAMP hydrolysis was similar from the two assays. Thus, the FRET-based PDE4 binding assay provides a convenient alternative approach to evaluate the structure−activity relationship of cAMP analogues and active-site-directed agents.

A higher specific FRET intensity was detected in the apoenzyme complex (ΔF_{max} ~ 110 intensity units) compared

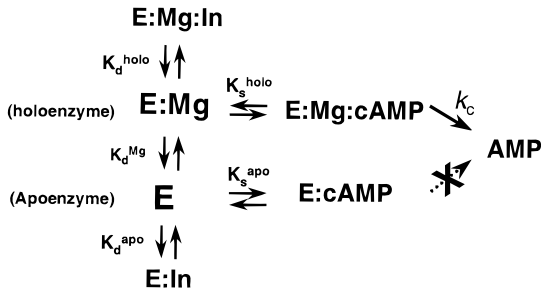

FIGURE 9: Scheme for cAMP and inhibitor binding to PDE4 apoenzyme and holoenzyme. K_d^{holo}, K_d^{apo}, K_s^{holo}, and K_s^{apo} are the dissociation constants of inhibior and cAMP with the PDE4 holoenzyme and apoenzyme, respectively. K_d^{Mg} is the dissociation constant of Mg^{2+} with the apoenzyme. k_c is the rate constant for cAMP hydrolysis.

Table 2: Comparison of cAMP Binding and Hydrolysis Using the FRET Binding Assay and PDE Activity Assay[a]

assay	parameter	apoenzyme	holoenzyme
FRET	binding affinity (IC_{50}, μM)	340 (±45)	3.8 (±0.4)
	estimated K_s (μM)	170 (±23)	1.9 (±0.2)
	turnover (s^{-1})	not detected	15
[^{3}H]-cAMP hydrolysis	K_m (μM)	−	2 (±0.5)
	k_{cat} (s^{-1})	not detected	9−17

[a] Results of the FRET binding assay were from Figure 8A−C. The K_s values for cAMP binding to holoenzyme (5 mM Mg^{2+}) and apoenzyme (10 mM EDTA) were estimated using $K_s = IC_{50}/(1 + [\text{L-791,760}]/K_d)$ where K_d is the binding affinity of L-791,760. The K_m and k_{cat} values were determined by monitoring the hydrolysis of [^{3}H]-cAMP (from 0 to 20 μM) to [^{3}H]-AMP in the presence of 10 mM Mg^{2+}. k_{cat} typically ranged from 9 to 17 s^{-1} (V_{max} from 5 to 10 μmol $mg^{-1}min^{-1}$) for different preparations of GST-PDE4A^{248}. No [^{3}H]-cAMP hydrolysis was detected with the apoenzyme after a 2 h incubation (10 mM EDTA, 10 μM [^{3}H]-cAMP, 50 nM enzyme).

with its holoenzyme complex ($\Delta F_{max} \sim 80$ intensity units) from extrapolating the binding curves in Figure 5. This was likely derived from a response difference between the two complexes. Either a more efficient energy transfer in the apoenzyme complex due to an altered dipole moment alignment of the PDE4 excited state with the bound L-791,-760 or a changed environment could account for the change in ΔF_{max} (Mg^{2+} had no detectable effect on the fluorescence spectrum of L-791,760). There is no evidence to suggest the presence of any additional binding. In addition to their monophasic binding curves, the uniform nature of the L-791,-760 interaction with either conformer was supported by the monophasic and complete displacement curves of cAMP and other inhibitors.

PDE4 catalysis requires the presence of a divalent metal cation such as Mg^{2+}, Co^{2+}, Zn^{2+}, Ni^{2+}, or Mn^{2+} (*31, 34, 35*). Structurally, the metal binding site is likely composed of one or both of the "Zn^{2+}-binding" amino acid motifs, conserved within the catalytic domains of mammalian PDEs. Their importance in both catalysis and inhibitor binding was confirmed from mutational studies on PDE3, PDE4, and PDE5 (*25, 37*−*39*). The EC_{50} value of Mg^{2+} in activating cAMP hydrolysis, which typically ranged from 0.1 to 1 mM for various PDE4s, was within its free intracellular concentration range of 0.3−0.7 mM, and suggests that Mg^{2+} is the endogenous cofactor (*11, 40*). In contrast, the EC_{50} values for Zn^{2+}, Mn^{2+}, and Co^{2+} as cofactors, which ranged from 0.5 to 5 μM, were above their known free physiological concentrations (low nanomolar; *31, 41*).

Theoretically, a catalytically essential metal cation could play one or several roles in activating the PDE catalytic machinery. It may act as a structural metal ion that induces the high-affinity binding of cAMP by either directly or indirectly interacting with it. Second, it may act as a catalytic metal ion that coordinates to the phosphate oxygens of cAMP to increase its chemical reactivity. A third role for the catalytic metal ion would be to chelate a water molecule to provide the catalytic hydroxide nucleophile near neutral pH. The stereochemistry of the PDE-mediated hydrolysis of cAMP proceeded with an inversion of configuration at the phosphate, consistent with an in-line attack by a metal-hydroxide (*42*). The identification of the weak ($K_d \sim 170$ μM) but presumably nonproductive cAMP/apoenzyme complex in the present study (no [^{3}H]-AMP production detected after 2 h incubation) demonstrated that the cofactor binding to PDE4 was responsible for inducing not only its high-affinity interaction with cAMP but also the activation of the catalytic machinery. These results are consistent with the hypothetical scheme in Figure 10 to account for the dual roles of the Mg^{2+} cofactor.

Contrary to Zn^{2+} hydrolases, PDE4−cofactor binding has been found to be rapidly reversible. PDE4A$^{1-886}$ purified in the presence of EDTA lacked any significant amount of divalent cations (<0.1 mol fraction) based on direct metal ion analysis. Its Zn^{2+} binding, close to stoichiometric in the absence of cAMP, had a K_d of 0.5 μM and a dissociation half-life of ~30 s (*31*). The dissociation rate of Zn^{2+} and the slow transition triggered by EDTA in Figure 7 both supported a slow association of Zn^{2+} or Mg^{2+} with the PDE4 apoenzyme. The estimated apparent k_{on} of $\sim 4 \times 10^4$ M^{-1} s^{-1} for Zn^{2+} binding to PDE4 apoenzyme, based on its 0.5 μM K_d, was several orders of magnitude slower than the commonly accepted diffusion rate of $\sim 10^9$ M^{-1} s^{-1} (*43*). The slow association between the cofactor and the apoenzyme signifies the presence of a structural reorganization of the residues involved. The Mg^{2+} binding to PDE4 apoenzyme was not accompanied by a detectable change in its intrinsic fluorescence, consistent with the absence of a global conformational change between the two conformers. Furthermore, the ability of both conformers to bind cAMP and some inhibitors implicated that the overall topology of the active site remains conserved with only limited area being perturbed by the presence of cofactor. Our results showing the selective binding of cAMP to the PDE4 holoenzyme differ from earlier reports of the random equilibrium binding of Mg^{2+} and cGMP to the cGMP-specific PDE5 and PDE6 (*44, 45*). This may reflect a difference between these PDEs.

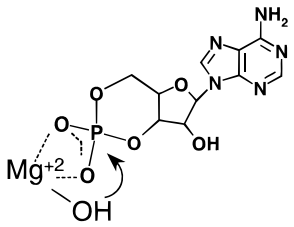

FIGURE 10: Scheme for Mg^{2+}-induced high-affinity cAMP binding and catalysis activation. The dual roles of Mg^{2+} are (a) enhancing cAMP binding and activating phosphate by chelating with the phosphate oxygens and (b) providing an activated hydroxyl nucleophile near neutral pH. It remains to be clarified whether they are fulfilled by a single metal ion as illustrated or by two nearby metal ions analogous to that found in adenylyl cyclase (*52*).

In addition to inducing the high-affinity cAMP binding and activating catalysis, the conformational difference between the two conformers influences the binding of inhibitors. This was first noted by Schneider and co-workers, who determined that Mg^{2+} was required for the high-affinity (*R*)-rolipram interaction with PDE4-containing rat brain membrane preparations (*46*). Percival and co-workers have also reported that the potencies of several competitive inhibitors, such as (*R*)-rolipram and CDP-840, were shifted in the presence of Zn^{2+} compared to their potencies in the presence of Mg^{2+} (*31*). Here we have demonstrated that inhibitors bind differentially to the apoenzyme and holoenzyme depending on their structures. A cofactor-dependent interaction dominated the binding of SB-207499, RP-73401, and CDP-840 to PDE4, whereas the binding of L-791,760 and RS-14203 with PDE4 relied heavily on a cofactor-independent interaction. In the absence of detailed structural information to confirm the hypothesis, it is still tempting to speculate that the cofactor-dependent interaction might involve the potential metal binding motifs, such as the vicinal dialkoxyphenyl moiety, common among many PDE4 inhibitors (*47*−*51*). The structure-dependent differential binding of inhibitors to the apoenzyme and holoenzyme offers an opportunity to selectively target inhibitors at one of the two conformations in vivo. However, it remains to be demonstrated whether this approach would provide any benefits.

The binding of Mg^{2+} to PDE4 has been shown to be upregulated by serine phosphorylation. A partially phosphorylated PDE4D3 exhibited a biphasic Mg^{2+} response curve with EC_{50} values at ~0.3 and >10 mM, respectively. Further phosphorylation by PKA on Ser^{54} in the conserved RRES motif converted the remaining low-affinity population into the high-affinity state, leading to activity activation and an

increased catalytic potency for (*R*)-rolipram (*11*). We have obtained similar results using a partially purified PDE4A$^{1-886}$ expressed in SF9 cells. The inhibitory potency of (*R*)-rolipram was shifted from ~120 to ~8 nM after treatment with PKA in the presence of 5 mM Mg^{2+}. A similar potency shift for (*R*)-rolipram was achieved without PKA treatment by increasing the Mg^{2+} concentration from 5 to 200 mM to favor holoenzyme formation. In addition to the regulation by phosphorylation, variable EC_{50} values for Mg^{2+} have been reported for several mutants of PDE4 that lacked the PKA activation site (*23*, *40*). These results support the hypothesis that the Mg^{2+} binding affinity in PDE4 is modulated readily, and this in turn leads to the regulation of its activity. This may represent an efficient regulatory machinery for controlling the cAMP-mediated processes through either phosphorylation or protein/protein interaction.

The differential binding of some inhibitors to both PDE4 apoenzyme and holoenzyme, coupled with the active binding of cAMP to the latter, complicates the kinetics of PDE4 inhibition. The kinetic consequence from the presence of the multiple enzyme species in Figure 9 is dictated by its rate-limiting transition, which remains to be resolved. Under the equilibrium assumption, the dual bindings of an inhibitor to both conformers lead to its catalytic potency to partition between its holoenzyme and apoenzyme affinities depending on the apoenzyme/holoenzyme ratio, with the IC_{50} value approaching its holoenzyme affinity under a saturating concentration of cofactor. This is consistent with the data listed in Table 1. In addition, the model predicts a shallow titration curve for inhibitors such as (*R*)-rolipram using a partially activated enzyme preparation, which is likely responsible for much of the reported behavior of (*R*)-rolipram (*23*). On the other hand, a rate-limiting exchange between its apoenzyme complex and its holoenzyme complex, in comparison with the cAMP turnover, would further complicate the titration curve for rolipram. The last scenario might be related to the time-dependent inhibition of PDE4B by (*R*)-rolipram (*28*). Thus, dissecting the transition times among the enzyme species becomes essential in further clarifying the remaining issues in the kinetic inhibition of PDE4. The formation and breakup of the FRET complexes, such as those in Figure 4, were too fast to be quantified using the current instrument setup. Further analysis of these transitions on a faster spectrophotometer may help to uncover some of the embedded rate constants.

In conclusion, we have developed a novel FRET-based equilibrium PDE4 binding assay, capable of monitoring the occupancy of the PDE4 active site continuously. We demonstrated that the Mg^{2+}-induced PDE4 conformational change is responsible for eliciting its high-affinity interaction with cAMP, the activation of catalysis, and the differential binding of inhibitors. High- and low-affinity (*R*)-rolipram bindings were detected owing to its differential interaction with the PDE4 holoenzyme and apoenzyme.

ACKNOWLEDGMENT

We thank Drs. Dave Percival, Ernest Asante-Appiah, and Brian Kennedy, Mr. James Mortimer, and Ms. Ellie James for helpful discussions and critical reading of the manuscript. Ms. Barbara Jardin at BRI is thanked for assistance with the production of GST-PDE4A^{248}.

REFERENCES

1. Soderling, S. H., Bayuga, S. J., and Beavo, J. A. (1999) *Proc. Natl. Acad. Sci. U.S.A. 96*, 7071−7076.
2. Fujishige, K., Kotera, J., Michibata, H., Yuasa, K., Takebayashi, Si, Okumura, K., and Omori, K. (1999) *J. Biol. Chem. 274*, 18438−18445.
3. Beavo, J. A., Conti, M., and Heaslip, R. J. (1994) *Mol. Pharmacol. 46*, 399−405.
4. Conti, M., Nemoz, G., Sette, C., and Vicini, E. (1995) *Endocr. Rev. 16*, 370−389.
5. Houslay, M. D., and Milligan, G. (1997) *Trends Biochem. Sci. 22*, 217−224.
6. Torphy, T. J. (1998) *Am. J. Respir. Crit. Care Med. 157*, 351−370.
7. Houslay, M. D., Scotland, G., Erdogan, S., Huston, E., Mackenzie, S., McCallum, J. F., McPhee, I., Pooley, L., Rena, G., Ross, A., Beard, M., Peder, A., Begg, F., and Wilkinson, I. (1997) *Biochem. Soc. Trans. 25*, 374−381.
8. Bolger, G. B., Erdogan, S., Jones, R. E., Loughney, K., Scotland, G., Hoffmann, R., Wilkinson, I., Farrell, C., and Houslay, M. D. (1997) *Biochem. J. 328*, 539−548.
9. Yarwood, S. J., Steele, M. R., Scotland, G., Houslay, M. D., and Bolger, G. B. (1999) *J. Biol. Chem. 274*, 14909−14917.
10. Salanova, M., Chun, S. Y., Iona, S., Puri, C., Stefanini, M., and Conti, M. (1999) *Endocrinology 140*, 2297−2306.
11. Sette, C., and Conti, M. (1996) *J. Biol. Chem. 71*, 16526−16534.
12. Hoffmann, R., Wilkinson, I. R., McCallum, J. F., Engels, P., and Houslay, M. D. (1998) *Biochem. J. 333*, 139−149.
13. Hoffmann, R., Baillie, G. S., MacKenzie, S. J., Yarwood, S. J., and Houslay, M. D. (1999) *EMBO J. 18*, 893−903.
14. Cherry, J. A., and Davis, R. L. (1999) *J. Comput. Neurol. 407*, 287−301.
15. Iona, S., Cuomo, M., Bushnik, T., Naro, F., Sette, C., Hess, M., Shelton, E. R., and Conti, M. (1998) *Mol. Pharmacol. 53*, 23−32.
16. Horowski, R., and Sastre-Y-Hernandez, M. (1998) *Curr. Ther. Res. 38*, 23−29.
17. Barnette, M. S., Grous, M., Cieslinski, L. B., Burman, M., Christensen, S. B., and Torphy, T. J. (1995) *J. Pharmacol. Exp. Ther. 273*,1396−1402.
18. Torphy, T. J., Barnette, M. S., Underwood, D. C., Griswold, D. E., Christensen, S. B., Murdoch, R. D., Nieman, R. B., and Compton, C. H. (1999) *Pulm. Pharmacol. Ther. 12*, 131−135.
19. Torphy, T. J., Stadel, J. M., Burman, M., Cieslinski, L. B., McLaughlin, M. M., White, J. R., and Livi, G. P. (1992) *J. Biol. Chem. 267*, 1798−1804.
20. Jacobitz, S., McLaughlin, M. M., Livi, G. P., Burman, M., and Torphy, T. J. (1996) *Mol. Pharmacol. 50*, 891−899.
21. Owens, R. J., Catterall, C., Batty, D., Jappy, J., Russell, A., Smith, B., O'Connell, J., and Perry, M. J. (1997) *Biochem. J. 326*, 53−60.
22. Perry, M. J., O'Connell, J., Walker, C., Crabbe, T., Baldock, D., Russell, A., Lumb, S., Huang, Z., Howat, D., Allen, R., Merriman, M., Walls, J., Daniel, T., Hughes, B., Laliberte, F., Higgs, G. A., and Owens, R. J. (1998) *Cell. Biochem. Biophys. 29*, 113−132.
23. McPhee, I., Yarwood, S. J., Scotland, G., Huston, E., Beard, M. B., Ross, A. H., Houslay, E. S., and Houslay, M. D. (1999) *J. Biol. Chem. 274*, 11796−11810.
24. Jin, S. L., Swinnen, J. V., and Conti, M. (1992) *J. Biol. Chem. 267*, 18929−18939.
25. Jacobitz, S., Ryan, M. D., McLaughlin, M. M., Livi, G. P., DeWolf, W. E., Jr., and Torphy, T. J. (1997) *Mol. Pharmacol. 51*, 999−1006.
26. Atienza, J. M., Susanto, D., Huang, C., McCarty, A. S., and Colicelli, J. (1999) *J. Biol. Chem. 274*, 4839−4847.
27. Rocque, W. J., Holmes, W. D., Patel, I. R., Dougherty, R. W., Ittoop, O., Overton, L., Hoffman, C. R., Wisely, G. B., Willard, D. H., and Luther, M. A. (1997) *Protein Expression Purif. 9*, 191−202.
28. Rocque, W. J., Tian, G., Wiseman, J. S., Holmes, W. D., Zajac-Thompson, I., Willard, D. H., Patel, I. R., Wisely, G. B., Clay,

W. C., Kadwell, S. H., Hoffman, C. R., and Luther, M. A. (1997) *Biochemistry 36,* 14250−14261.
29. Han, Y., Giroux, A., Lépine, C., Laliberté, F., Huang, Z., Perrier, H., Bayly, C., and Young, R. (1999) *Tetrahedron 55,* 11669−11685.
30. Perkins, S. J. (1986) *Eur. J. Biochem. 157,* 169−180.
31. Percival, M. D., Yeh, B., and Falgueyret, J. P. (1997) *Biochem. Biophys. Res. Commun. 241,* 175−180.
32. Perrier, H., Bayly, C., Laliberte, F., Huang, Z., Rasori, R., Robichaud, A., Girard, Y., and Macdonald, D. (1999) *Bioorg. Med. Chem. Lett. 9,* 323−326.
33. Lakowicz, J. R. (1983) *Principles of Fluorescence Spectroscopy,* pp 305−337 and pp 189−211, Plenum Press, New York.
34. Wilhelm, R. S., Fatheree, P. R., and Chin R. L. (1994) Patent WO9422852.
35. Donnelly, T. E., Jr. (1978) *Biochim. Biophys. Acta 522,* 151−160.
36. Kovala, T., Sanwal, B. D., and Ball, E. H. (1997) *Biochemistry 36,* 2968−2976.
37. Francis, S. H., Colbran, J. L., McAllister-Lucas, L. M., and Corbin, J. D. (1994) *J. Biol. Chem. 269,* 22477−22480.
38. Omburo, G. A., Brickus, T., Ghazaleh, F. A., and Colman, R. W. (1995) *Arch. Biochem. Biophys. 323,* 1−5.
39. Omburo, G. A., Jacobitz, S., Torphy, T. J., and Colman, R. W. (1998) *Cell. Signalling 10,* 491−497.
40. Saldou, N., Obernolte, R., Huber, A., Baecker, P. A., Wilhelm, R., Alvarez, R., Li, B., Xia, L., Callan, O., Su, C., Jarnagin, K., and Shelton, E. R. (1998) *Cell. Signalling 10,* 427−440.
41. Romani, A., and Scarpa, A. (1992) *Arch. Biochem. Biophys. 298,* 1−12.
42. Burgers, P. M., Eckstein, F., Hunneman, D. H., Baraniak, J., Kinas, R. W., Lesiak, K., and Stec, W. J. (1997) *J. Biol. Chem. 254,* 9959.
43. Fersht, A. (1985) *Enzyme structure and mechanism,* 2nd ed., W. H. Freeman and Company, New York.
44. Francis, S. H., Thomas, M. K., and Corbin, J. D. (1990) *Cyclic nucleotide phosphodiesterases: Structure, regulation and drug action* (Beavo, J., and Houslay, M. D., Eds.) pp 118−140, John Wiley & Sons Ltd., New York.
45. Srivastava, D., Fox, D. A., and Hurwitz, R. L. (1995) *Biochem. J. 308,* 653−658.
46. Schneider, H. H., Schmiechen, R., Brezinski, M., and Seidler, J. (1986) *Eur. J. Pharmacol. 27,* 105−115.
47. Charpiot, B., Brun, J., Donze, I., Naef, R., Stefani, M., and Mueller, T. (1998) *Bioorg. Med. Chem. Lett. 8,* 2891−2896.
48. Christensen, S. B., Guider, A., Forster, C. J., Gleason, J. G., Bender, P. E., Karpinski, J. M., DeWolf, W. E., Jr., Barnette, M. S., Underwood, D. C., Griswold, D. E., Cieslinski, L. B., Burman, M., Bochnowicz, S., Osborn, R. R., Manning, C. D., Grous, M., Hillegas, L. M., Bartus, J. O., Ryan, M. D., Eggleston, D. S., Haltiwanger, R. C., and Torphy, T. J. (1998) *J. Med. Chem. 41,* 821−835.
49. Dal Piaz, V., Giovannoni, M. P., Castellana, C., Palacios, J. M., Beleta, J., Domenech, T., and Segarra (1997) *J. Med. Chem. 40,* 1417−1421.
50. He, W., Huang, F. C., Hanney, B., Souness, J., Miller, B., Liang, G., Mason, J., and Djuric (1998) *J. Med. Chem. 41,* 4216−4223.
51. Montana, J. G., Buckley, G. M., Cooper, N., Dyke, H. J., Gowers, L., Gregory, J. P., Hellewell, P. G., Kendall, H. J., Lowe, C., Maxey, R., Miotla, J., Naylor, R. J., Runcie, K. A., Tuladhar, B., and Warneck, J. B. (1998) *Bioorg. Med. Chem. Lett. 8,* 2635−2640.
52. Tesmer, J. J., Sunahara, R. K., Johnson, R. A., Gosselin, G., Gilman, A. G., and Sprang, S. R. (1999) *Science 285* (5428), 756−760.

BI992432W